JOURNAL OF Applied Polymer SCIENCE

Synthesis, Characterization of Biomimetic Phosphorylcholine-Bound Chitosan Derivative and *In Vitro* Drug Release of Their Nanoparticles

Zehu Wang, Rong Zeng, Mei Tu, Jianhao Zhao
Department of Materials Science and Engineering, College of Science and Engineering, Jinan University, Guangzhou 510632, People's Republic of China
Correspondence to: R. Zeng (E-mail: tzengronga@jnu.edu.cn)

ABSTRACT: Novel water-soluble biomimetic phosphorylcholine (PC)—bound chitosan derivatives (*N*-PCCs) with different degree of substitution (DS) via a phosphoramide linkage between glucosamine and PC were synthesized through Atherton-Todd reaction under the mild conditions, and structurally characterized by ^{1}H-NMR, Fourier transform infrared (FTIR) spectroscopy, gel permeation chromatography (GPC), X-ray diffraction (XRD), differential scanning calorimetry (DSC) and thermal gravimetric analysis (TGA). Their DS ranged from $\sim$ 16 to $\sim$ 42 mol % based on the ^{1}H-NMR spectra. All these *N*-PCCs with decreased crystallization showed excellent solubility in the aqueous solutions within a wide pH range (1–12). DSC and TGA results revealed that the thermal stability of *N*-PCCs decreased with the increase of DS value. Further, *N*-PCCs nanoparticles could be still formed in a spherical shape similar to chitosan nanoparticles by ionic gelation technique, observed by atomic force microscopy (AFM). Dynamic light scattering (DLS) results suggested that the zeta potential value of *N*-PCCs nanoparticles decreased with the DS value increasing. Using 5-fluorouracil (5-Fu) as a model drug, *in vitro* drug release studies indicated that *N*-PCCs nanoparticles exhibited a similar prolonged release profile as chitosan nanoparticles. The results suggested that *N*-PCCs nanoparticles could be used as promising nanocarriers for drug delivery applications. © 2012 Wiley Periodicals, Inc. J. Appl. Polym. Sci. 000: 000–000, 2012

KEYWORDS: chitosan; phosphorylcholine; biomimetic; nanoparticle; drug release

Received 28 November 2011; accepted 1 June 2012; published online
DOI: 10.1002/app.38151

INTRODUCTION

Chitosan, derived from chitin, a linear polysaccharide mainly composed of 2-amino-2-deoxy-β-D-glucopyranose (D-glucosamine) residues, has a chemical structure similar to glycosaminoglycan in the extracelluar matrix (ECM). Recently, chitosan has attracted more and more attention in biomedical fields due to its biocompatibility, biodegradability, low immunogenicity and non-toxicity, including wound-dressing materials, scaffolds for tissue engineering, delivery systems for drug and gene.[1,2] However, chitosan is a highly crystalline material with a strongly hydrogen-bonded network structure and is insoluble in neutral aqueous solutions, which restricts its biomedical applications.[3] To overcome the limitation of poor solubility in neutral aqueous solutions, various chemical modification of chitosan have been developed, such as carboxymethylation,[4] quaternization,[5] succinic acylation,[6] thiolation,[7] sulfation,[8] and PEGylation.[9] Moreover, these synthesized chitosan derivatives with increased water-solubility showed some attractive physicochemical and biological properties for their pharmaceutical applications. For example, *N*-trimethyl chitosan chloride (TMC)[10] and thiolated chitosan[7] with mucoadhesive and permeation enhancing properties could be used as absorption enhancers for improved preoral delivery of peptide drugs. Sulfated chitosan derivatives with selective sulfation at *O*-2 and/or *O*-3 site showed a specific anti-AIDS activity without anticoagulant activity, while 6-*O*-sulfated chitosan derivative strongly inhibited blood coagulation.[8] *N*-succinyl-chitosan showing systemic long-circulation could be used as a drug carrier in cancer chemotherapy.[11]

Phosphorylcholine (PC) is a zwitterionic head group that is present in the outer leaflet of the lipid bilayer of red blood cell membranes (the major component of the extracellular side of cell membranes) in the form of the phospholipid, phosphatidylcholine.[12] Numerous studies have proven that the introduction of zwitterionic PC groups can improve not only the hydrophilicity of polymers but also their biocompatibility.[13–15] In particular, constructing biomembrane-like PC-containing polymers provided an alternative biomimetic strategy for preventing non-specific protein adsorption on the drug carriers to avoid the undesired biological response, e.g. the rapid clearance by the natural defence mechanisms of the body.[16–18] Many attempts

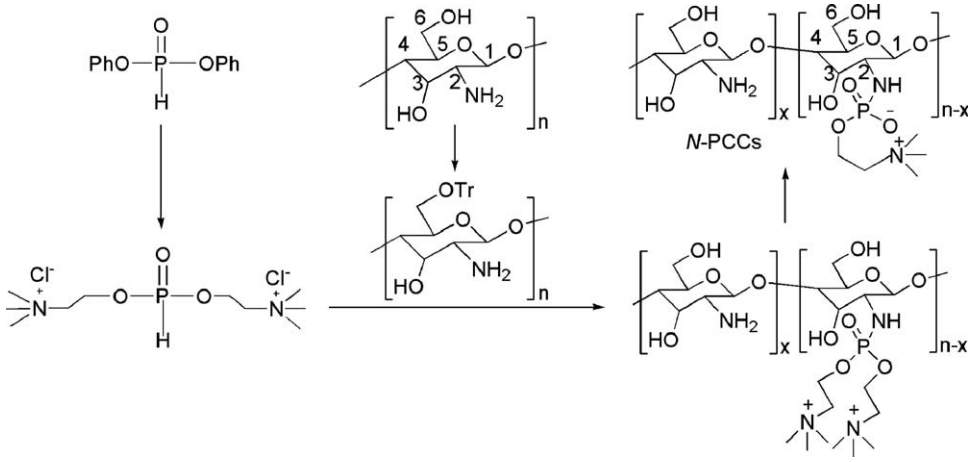

Scheme 1. Synthesis route of *N*-PCCs.

have been made in biomimetic modification of chitosan with PC moieties for improving its water-solubility and biocompatibility. Tiera et al.[19] reported the synthesis of PC-substituted chitosan derivatives soluble in physiological pH conditions by reductive amination of PC-glyceraldehyde with primary amines of chitosan. Meng et al.[20] synthesized PC-modified chitosan with excellent hemocompatibility and cytophilicity using 2-chloro-2-oxo-1,3,2-dioxaphospholane (COP).

In this article, we report the synthesis of biomimetic PC-bound chitosan derivatives (*N*-PCCs) with different degree of substitution (DS) via a phosphoramide linkage between glucosamine and PC through Atherton-Todd reaction under the mild conditions.[21] Their structure, thermal properties and water-solubility were evaluated by ^{1}H-NMR, Fourier transform infrared (FTIR) spectroscopy, gel permeation chromatography (GPC), X-ray diffraction (XRD), differential scanning calorimetry (DSC) and thermal gravimetric analysis (TGA), UV-vis spectroscopy. Since chitosan nanoparticles can be easily formed by ionic gelation technique for efficiently delivering drugs and other biologically active components, such as peptides, proteins and oligonucleotides,[2] we also investigated physicochemical properties of *N*-PCCs nanoparticles formed by ionically crosslinking with tripolyphosphate (TPP) by atomic force microscopy (AFM) and dynamic light scattering (DLS), and subsequently their drug loading and *in vitro* drug release behaviors using the anti-cancer drug 5-fluorouracil (5-Fu) as model drug.[22]

MATERIALS AND METHODS

Materials

Chitosan (low molecular weight, Brookfield viscosity: 20 cps) was purchased from Sigma-Aldrich Chemicals, then treated with 40% aqueous sodium hydroxide at 110°C for 1.5 h three times and purified before using. Diphenyl phosphate was also purchased from Sigma-Aldrich Chemicals. Choline chloride was purchased from J&K Chemical Company and was dried at elevated temperature in vacuum. 5-fluorouracil was obtained from Alfa Aesar Chemical Company. Other solvents were all commercially available reagents of analytical grade, dried and purified by distillation before using.

Synthesis of *N*-PCCs

The reaction scheme for the synthesis of *N*-PCCs is shown in Scheme 1. The procedure for the synthesis of *N*-PCCs42 is illustrated below. All experiments involving water-sensitive compounds were conducted under dry conditions. 6-*O*-trityl chitosan was firstly synthesized from chitosan in three steps, *N*-phthaloylation, 6-*O*-trityl protection and de-phthaloylation, according to the known procedure reported by Nishimura et al.,[23] which exhibited the excellent solubility in some organic solvents. Seven hundred and thirty-two milligram (5.2 mmol) of choline chloride was added to 0.475 mL (2.5 mmol) of diphenyl phosphite in 10 mL of freshly distilled pyridine/DMSO (1:10) at room temperature; the solution was stirred for 2 h. The crude product of dicholinyl H-phosphonate dichloride was obtained after the solvent was evaporated. Then it was dissolved in 10 mL of 2-propanol, and the solution was added dropwise to 6-*O*-trityl chitosan (200 mg, 0.50 mmol of free NH_2) in a mixed solution of dimethylacetamide (DMA, 10 mL), triethylamine [1.05 mL (7.5 mmol)], and tetrachloromethane [0.475 mL (5.0 mmol)] in ice-water bath. After stirring overnight, the resulting solution was evaporated to dryness, 10 mL of formic acid was added to the residue, and the solution was stirred for 1 h. Formic acid was removed by rotary evaporation, and the residue was dissolved in 5% $NH_3{\cdot}H_2O$ (20 mL). The solution was stirred for 2 h and then centrifuged at 5000 rpm at 20°C for 15 min. The supernatant from the centrifugation was dialyzed with distilled water for 3 day and lyophilized to provide the target product, *N*-PCCs42 (118 mg).

Other PC-bound chitosan derivatives with different DS were prepared following the same procedures except for the feed ratio of the reactants (Table I).

Characterization of *N*-PCCs

^{1}H-NMR. The ^{1}H-NMR spectra of chitosan and *N*-PCCs were determined on a Bruker UX-400 NMR spectrometer (Germany) at 400 MHz using 2% (v/v) CF_3COOD/D_2O as solvent. The degree of substitution (DS) of PC moiety was calculated by the amount ratio of H of $-N^+(CH_3)_3$ (from PC) to H1 (from glucosamine units of GlcN and GlcN-PC).

FTIR. IR spectra of chitosan and *N*-PCCs were recorded over the range of 400–4000 cm^{-1} on a Bruker Equinox-55 FTIR

Table I. Preparation Conditions and Physicochemical Properties of PC-Bound Chitosan Derivatives

Samples	Feed ratio[a]	DS (mol %)[b]	Yield (%)	M_w (g/mol)[c]	M_n (g/mol)[c]	M_w/M_n
Chitosan				2.9×10^4	1.8×10^4	1.61
N-PCCs16	1 : 1	16	75.8	1.8×10^4	0.72×10^4	2.50
N-PCCs27	2 : 1	27	91.2	2.5×10^4	0.98×10^4	2.55
N-PCCs42	5 : 1	42	89.4	2.2×10^4	0.89×10^4	2.47

[a]Mole ratio of dicholinyl H-phosphonate dichloride to NH_2 of trityl-chitosan.
[b]Degree of substitution (DS) of PC moiety, determined from ^{1}H-NMR measurements.
[c]Estimated from GPC measurement.

spectrometer (Germany) using samples which were mixed with KBr and then pressed to pellets.

GPC. The molecular weights and polydispersity (M_w/M_n, M_w = weight-average molecular weight, M_n = number-average molecular weight) of the samples were recorded on a GPC system (Waters 515-410, Column: Ultrahydrogel 250) using 0.1 mol/L AcOH/0.1 mol/L NaAc as the eluent at 40°C with a flow rate of 1.0 mL/min. The column system was calibrated by a set of monodispersed standard PEO.

XRD. Powder XRD patterns of chitosan and *N*-PCCs were measured using a Bruker D8 Focus X-ray diffractometer (Germany) with Cu Kα radiation at a generator voltage of 36 kV and a generator current of 20 mA. Samples were scanned from 2θ = 5–40° at a scanning rate of 8°/min.

DSC. The DSC thermograms of chitosan and *N*-PCCs were characterized on a differential scanning calorimeter (NETZSCH DSC 204F1 Phoenix, Germany) in a temperature range from 20 to 400°C under nitrogen atmosphere with a heating rate of 10°C/min.

TGA. The thermal gravimetric analysis of chitosan and *N*-PCCs was implemented using TGA thermal analyzer (NETZSCH TG 209F3 Tarsus, Germany). The analysis was preformed under continuous flow of dry nitrogen gas at a heating rate of 10°C/min in a temperature range from 20 to 500°C.

Turbidity Measurements

To assess the water solubility of *N*-PCCs samples, changes of the transmittance at λ = 566 nm of aqueous *N*-PCCs solutions (4.0 g/L) were monitored within a wide pH range (1–12) using a Daojin UV-2550 UV-vis spectrometer (Japan). Samples were dissolved in HCl (0.1 mol/L) and titrated with an aqueous NaOH solution (4 mol/L). The solution pH was measured with a METTLER TOLEDO pH-meter.

Preparation of Chitosan and *N*-PCCs Nanoparticles

Chitosan and *N*-PCCs nanoparticles were prepared according to the procedure reported by Calvo et al.[24] In short, 9 mg chitosan or *N*-PCCs was dissolved in 2% (w/v) acetic solution at 1 mg/mL. Under magnetic stirring at 800 rpm at room temperature, 3 mL TPP aqueous solution (0.1% w/v) was added dropwise into the chitosan solution or *N*-PCCs solutions through a syringe needle (0.45 mm in diameter), and stirred continuously for 1 h to stabilize the nanoparticles through the electrostatic interaction with TPP.

Physicochemical Characterization of the Nanoparticles

Morphology of the Nanoparticles. The morphological characteristics of the nanoparticles were examined using Atomic Force Microscopy (AFM) (Bioscope catalyst). one drop of freshly made nanoparticles solution were dripped on a freshly cleaved mica surface, predried in the air for 1 h, and then dried in desiccator.

Particle size and Zeta Potential of the Nanoparticles. The particle size, polydispersity (size distribution) and zeta potential of the freshly prepared nanoparticles were measured using a Malvern 3000HSA Zetasizer based on the Dynamic Light Scattering (DLS) techniques. All DLS measurements were done with a wavelength of 633 nm at 25°C with an angle detection of 90°.

Drug loading and *In Vitro* Release

5-Fu-loaded chitosan and *N*-PCCs nanoparticles were prepared by premixing 5-Fu (0.5 mg/mL) with chitosan and *N*-PCCs27 acetic aqueous solution and then following above procedure. Afterwards, the nanoparticles were obtained by centrifugal separation, washed with acetone for three times and dried under vacuum overnight until constant weight. The encapsulation efficiency and loading capacity of nanoparticles were determined by the separation of nanoparticles from the aqueous medium containing free drug by ultra centrifugation at 20,000 rpm for 30 min. The amount of free 5-Fu in the supernatant was measured by Daojin UV-2550 UV-vis spectrometer (Japan) at 266 nm. The 5-Fu loading capacity of the nanoparticles and the 5-Fu encapsulation efficiency of the process were calculated with eqs. (1) and (2):

$$\text{5-Fu loading capacity} = (\text{A} - \text{B})/\text{C} \times 100 \quad (1)$$

$$\text{5-Fu encapsulation efficiency} = (\text{A} - \text{B})/\text{A} \times 100 \quad (2)$$

where A is the total amount of 5-Fu, B is the free amount of 5-Fu, and C is the nanoparticle weight. Each experiment was performed in triplicate.

For the *in vitro* release experiments, 50 mg 5-Fu-loaded nanoparticles were placed in the dialysis bag and suspended in 200 mL PBS solution (pH 7.4), incubated on a shaking water-bath at 100 rpm at 37.0°C. Aliquots of the dissolution medium (2 mL) were withdrawn at predetermined time intervals and replaced by fresh buffer to maintain a constant volume of releasing medium. The amount of released 5-Fu was determined by UV-vis spectrophotometric measurements at 266 nm. Each experiment was repeated in triplicate.

Applied Polymer SCIENCE

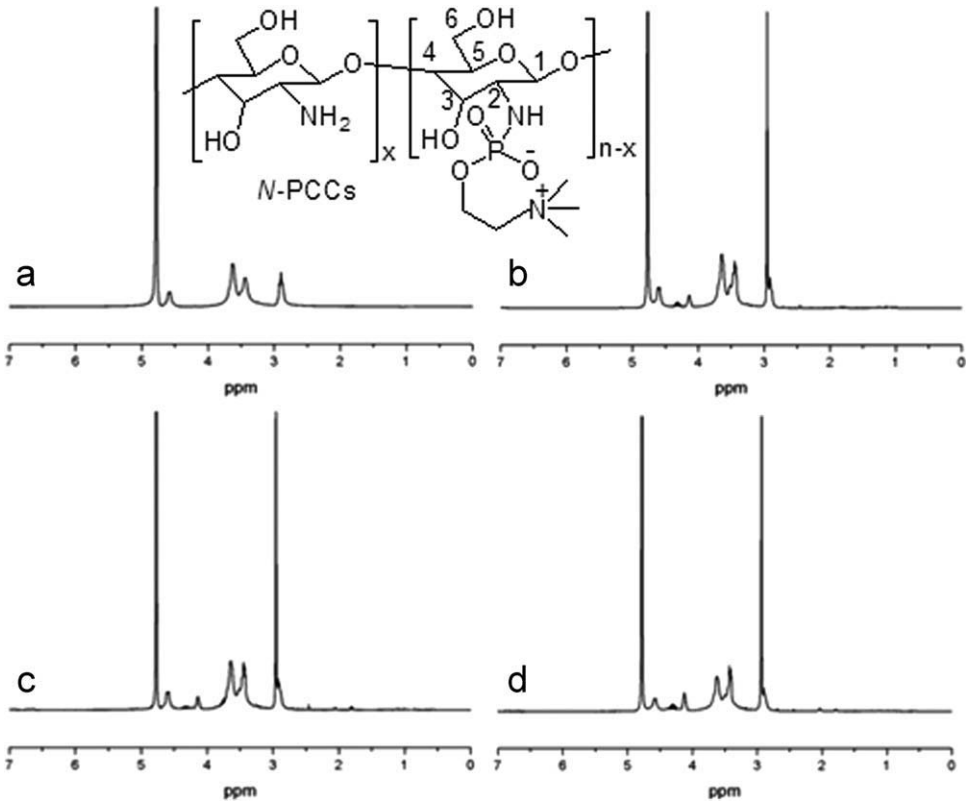

Figure 1. ^{1}H-NMR spectra of (a) chitosan, (b) *N*-PCCs16, (c) *N*-PCCs27, (d) *N*-PCCs42.

RESULTS AND DISCUSSION

Synthesis and Characterization of *N*-PCCs

To our knowledge, Atherton-Todd reaction is an efficient method for the construction of phosphoramidates from H-phosphates. In this work, we successfully coupled PC groups to chitosan backbone via a phosphoramide linkage through Atherton-Todd reaction. The reaction scheme and the chemical structure of PC-bound chitosan derivative are given in Scheme 1. The DS of PC on chitosan could be controlled by adjusting the feed ratio of the reactants. The ^{1}H-NMR spectra was used for both the chemical structure confirmation and the DS determination of *N*-PCCs. For pure chitosan [Figure 1(a)], the peaks at 4.61 ppm and 2.89 ppm were the signals of H1 and H2, respectively; the peaks from 3.42 to 3.73 ppm were attributed to H3, H4, H5, and H6 protons (labeled in Scheme 1). Compared with the pure chitosan, the *N*-PCCs [Figure 1(b–d)] exhibited a new strong peak at 2.96 ppm, assigned to hydrogen protons of $N^{+}(CH_3)_3$; and a small peak at 4.19 ppm corresponding to the methylene protons of $N^{+}(CH_3)_3$—CH_2—CH_2—. The changes indicate that the PC moiety has been conjugated to the amino group of the chitosan. And the corresponding DS value of PC of *N*-PCCs was calculated by the amount ratio of H of —$N^{+}(CH_3)_3$ (from PC) to H1 (from glucosamine units of GlcN and GlcN-PC), ranged from 16 to 42 mol % listed in Table I. The results clearly confirmed that *N*-PCCs with different DS value could be obtained by Atherton-Todd reaction, though the conversion rate of dicholinyl H-phosphonate to phosphoramidate was relatively low, which may be mainly attributable to the steric hindrance of trity1-chitosan derivative.

FTIR Characterization

The chemical structure of chitosan and *N*-PCCs were also analyzed using FTIR spectroscopy, confirming the linking of PC onto chitosan. Figure 2 shows the FTIR spectra of samples. The FTIR spectrum of chitosan [Figure 2(a)] showed a broad absorption band ascribed to the stretching vibration of —NH_2 and —OH group at 3300–3500 cm^{-1} and the aliphatic C–H stretch band between 2800 and 2990 cm^{-1}. The adsorption

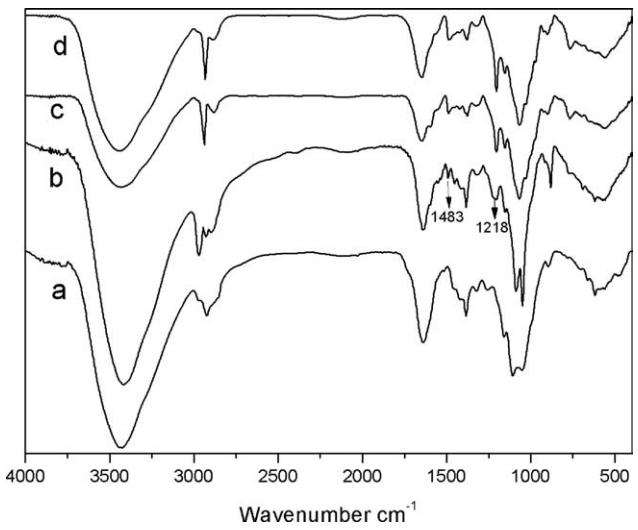

Figure 2. FTIR spectra of (a) chitosan, (b) *N*-PCCs16, (c) *N*-PCCs27, (d) *N*-PCCs42.

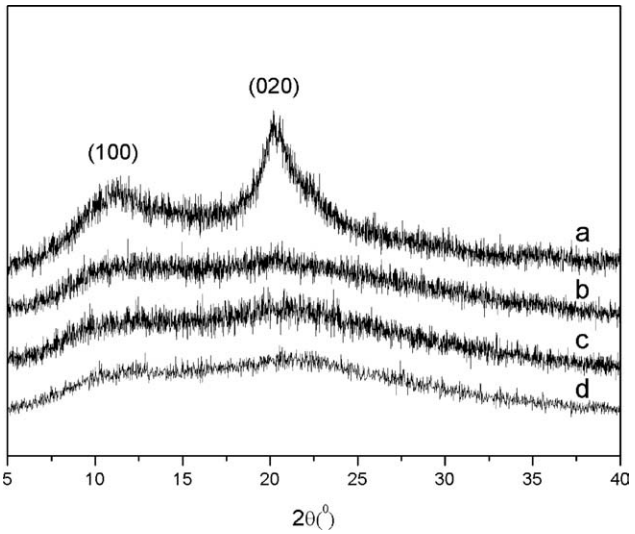

Figure 3. XRD Patterns of (a) chitosan, (b) *N*-PCCs16, (c) *N*-PCCs27, (d) *N*-PCCs42.

peak at 1637 cm^{-1} could be attributed to amide I of chitosan, the peak at 1385 cm^{-1} corresponded to the –C–O stretch of primary alcoholic group (—CH_2—OH),[25] and the absorption bands at 1000–1200 cm^{-1} were attributed to its saccharine structure. Compared with that of pure chitosan, the FTIR spectra of *N*-PCCs samples [Figure 2(b–d)] presented two new peaks at 1483 cm^{-1} corresponding to the bending of $N^+(CH_3)_3$, and at 1218 cm^{-1} ascribed to the asymmetric stretching of O=P—O,[26] which provided further evidence for the successful incorporation of PC moieties onto the chitosan backbone.

The molar masses of the samples obtained by GPC analysis are also summarized in Table I. It is found that *N*-PCCs appeared lower *Mw* values but higher *Mw/Mn* values compared with the starting chitosan, suggesting that main chain degradation took place during the chemical modification of chitosan. Since the conditions of coupling PC groups to trity1-chitosan by Atherton-Todd reaction were quite mild, chitosan chain scission occurred mostly during the regioselective protection and deprotection process of chitosan.[23]

XRD Analysis

Figure 3 demonstrates the XRD patterns of *N*-PCCs as compared with that of chitosan. The pure chitosan exhibited two obvious broad diffraction peaks at 2θ of 10.3 and 20.1° corresponding to the respective equatorial (100) and (020) reflections of the L-2 polymorph of chitosan reported previously.[27] However, these two characteristic peaks almost disappeared in the XRD curves of *N*-PCCs with three different DS, indicating that the introduction of the PC moieties onto chitosan had destroyed the crystallinity of the chitosan backbone and all three *N*-PCCs samples could be amorphous. Actually, the ordered crystalline structures of chitosan are stabilized by intra- and intermolecular hydrogen bonds, chemical modification of chitosan may prevent hydrogen bonding (H-bond) to suppress the formation of crystalline structure.[28] Zhang et al.[29] reported that *O*-succylation of chitosan decreased its ability of forming intermolecular hydrogen bonds and resulted in *O*-succinyl-chitosan becoming amorphous. It can be expected that the physicochemical properties of *N*-PCCs, such as thermal properties and solubility, would be greatly affected due to the alteration of the phase structure as compared with that of chitosan.

Thermal Properties

The thermal behavior of chitosan and *N*-PCCs was examined with DSC and TGA measurements. Figure 4 shows the first-heating DSC curves of chitosan and *N*-PCCs. The DSC thermograms of chitosan showed a broad endothermic peak around 67°C and a sharp exothermic peak at 311°C. The former endothermic peak might be due to the vaporation of the bound water in chitosan, while the latter might be attributed to the thermal decomposition of chitosan. In general, polysaccharides have a strong affinity for water and can be easily hydrated in the solid state, and their changes in chemical and physical structures also have a strong influence on the evaporation behavior of bound water. The DSC results of *N*-PCCs with different DS value showed broad endothermic peaks around 75–100°C higher than pure chitosan, which might be due to the loss of water adsorbed in the polysaccharides, suggesting that the introduction of PC moieties onto chitosan backbone could increase their affinity for water. Moreover, the exothermic peaks for *N*-PCCs16, *N*-PCCs27, and *N*-PCCs42 corresponding to their decomposition shifted towards lower temperature at 268°C, 258°C, and 247°C, respectively. The results indicated that the content of PC moieties plays a significant role in the decomposition of *N*-PCCs derivatives.

Thermographs of the chitosan and *N*-PCCs derivatives are shown in Figure 5. All the samples showed two obvious stages of weight loss. The slow weight loss with a temperature below 100°C was attributed to the evaporation of absorbed water, and the value of weight loss increased with an increase of DS value, probably due to the corresponding increased hydrophilicity of *N*-PCCs. The fast weight loss with a temperature above 200°C was due to the decomposition of the polymers. For the

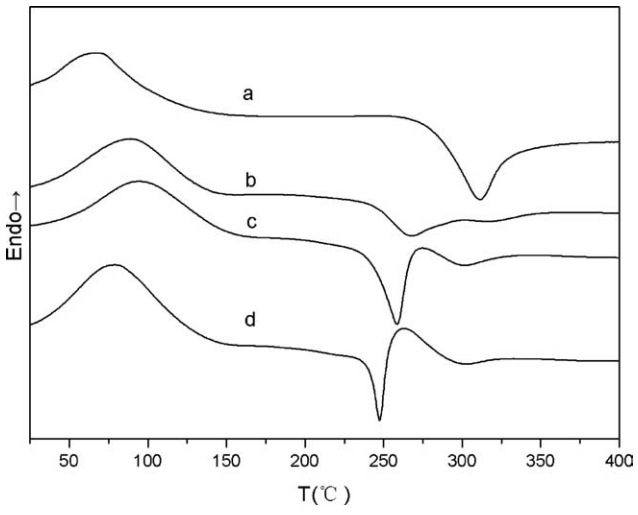

Figure 4. First-Heating DSC Patterns of (a) chitosan, (b) *N*-PCCs16, (c) *N*-PCCs27, (d) *N*-PCCs42.

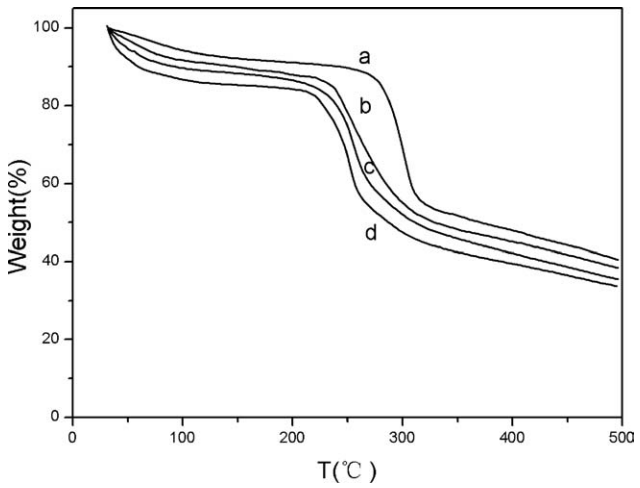

Figure 5. Thermogravimetric curves of (a) chitosan, (b) *N*-PCCs16, (c) *N*-PCCs27, (d) *N*-PCCs42.

N-PCCs, the decomposition temperature decreased with an increase of DS, which was in agreement with the result of DSC measurements as described above. These data also coincided well with the above XRD analysis for chitosan and *N*-PCCs. It can be concluded that the incorporation of PC groups into polysaccharide structures could disrupt the crystalline structure of chitosan and reduce its thermal stability, especially through the loss of the hydrogen bonding.[29,30]

Solubility of Samples in Aqueous Solutions

To assess the effect of the PC moieties coupling on the solubility of *N*-PCCs samples in neutral aqueous solutions, we monitored the changes in transmittance at $\lambda = 566$ nm of aqueous polymer solutions with a wide pH range (1–12) (Figure 6). All *N*-PCCs samples, as well as chitosan, were soluble in acidic conditions (pH < 6.0). Solutions of *N*-PCCs samples with DS 16, 27, and 42% remained transparent to light (almost 100% transmittance) independently of pH, whereas the transmittance of the chitosan solution decreased sharply for solutions of pH > 6.5. Linking PC moieties to poorly water soluble chitosan resulted in a significant enhancement of its water solubility even in strongly alkaline solutions, a direct consequence of the zwitterionic nature of PC moieties[18] and the amorphous structure of *N*-PCCs.

Nanoparticle Characterization

Figure 7 shows AFM images of chitosan and *N*-PCCs nanoparticles formed under the same conditions. As shown in Figure 6(a), the chitosan nanoparticles appeared spherical shape, Figure 6(b–d) illustrated that the *N*-PCCs nanoparticles formed under the same conditions had similar spherical structure. The results suggested that *N*-PCCs nanoparticles could be still formed by the same complexation mechanism mainly based on the ionic gelation interaction between the positively charged NH_3^+ and negatively charged TPP as chitosan nanoparticles.

The characteristics of the chitosan nanoparticles and the *N*-PCCs nanoparticles are summarized in Table II. Chitosan nanoparticles showed an average hydrodynamic diameter of 165 nm with PDI 0.319, and had a positive zeta potential of about +42 mV. Compared with chitosan nanoparticles, the size of *N*-PCCs nanoparticles decreased to some extent, but did not show distinct regularity. The particle size from AFM was smaller than that from DLS, which was mainly due to the process involved in the preparation of the samples. It was known that the AFM gave the images of the particles in the dry state, while DLS depicted the value of the nanoparticle size in solution of the sample. The size determined by DLS included hydrated layers surrounding the nanoparticles, and was therefore larger than that in dry state determined by AFM. In addition, the zeta potential of the *N*-PCCs nanoparticles decreased as the DS increased, because electrically neutral zwitterionic PC groups existed in the surface of *N*-PCCs nanoparticles.

Drug Loading and *In Vitro* Release

It has been widely accepted that the ionically crosslinked chitosan nanoparticles with TPP are efficient nanocarriers for delivering therapeutic and/or diagnostic agents. In this work, according to the UV-vis data, the *N*-PCCs27 nanoparticles exhibited similar encapsulation efficiency and loading capacity for 5-Fu as the chitosan nanoparticles formed under the same conditions. The 5-Fu encapsulation efficiency and loading capacity were 85.2% and 33.3% for chitosan nanoparticles, 83.6% and 35.8% for *N*-PCCs27 nanoparticles, respectively. The results indicated that the 5-Fu loading process was almost not influenced by the introduction of PC groups on the chitosan backbone. The 5-Fu *in vitro* release behaviors of the chitosan and *N*-PCCs27 nanoparticles in PBS at 37.0°C are shown in Figure 8. As can be seen, both release profiles of the chitosan and *N*-PCCs27 nanoparticles were similar, exhibiting a burst release in the first 5 h, and followed by a slow release, but the release rate of 5-Fu from *N*-PCCs27 nanoparticles was slightly higher than that of chitosan nanoparticles due to their improved hydrophilicity. The initial burst release was mainly caused by diffusion of 5-Fu located closer to the surface of nanoparticles, and the second period was possibly related to the gradual degradation of the

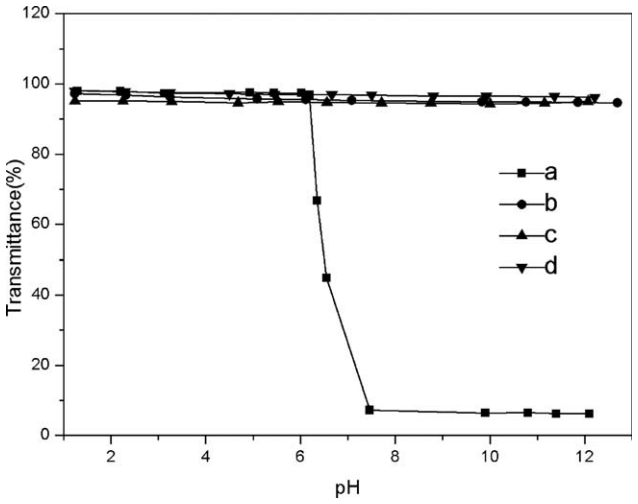

Figure 6. Changes with pH of the Transmittance of (a) chitosan, (b) *N*-PCCs16, (c) *N*-PCCs27, (d) *N*-PCCs42.

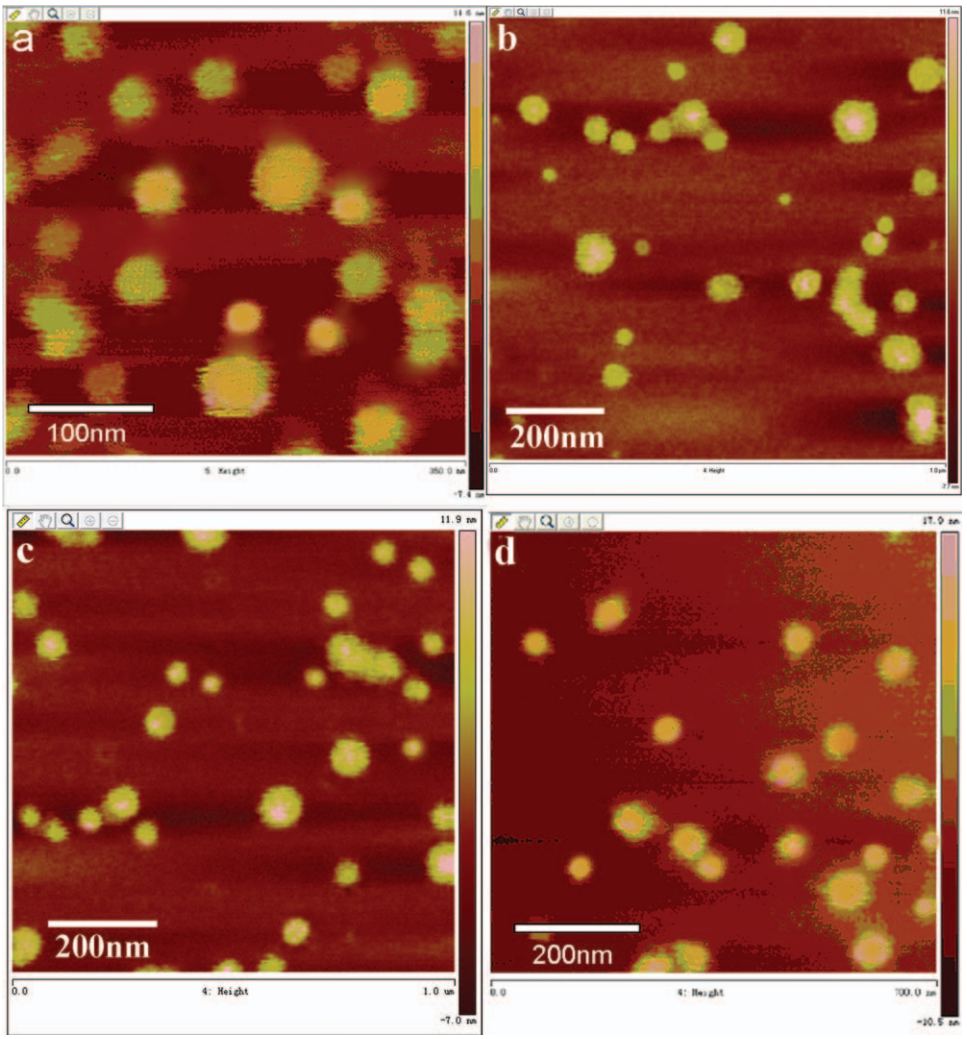

Figure 7. AFM images of (a) chitosan nanoparticles, (b) *N*-PCCs16 nanoparticles, (c) *N*-PCCs27 nanoparticles, (d) *N*-PCCs42 nanoparticles. [Color figure can be viewed in the online issue, which is available at wileyonlinelibrary.com.]

nanoparticles.[31] The results suggested that *N*-PCCs nanoparticles may provide a prolonged release of drugs in physiological conditions as chitosan nanoparticles. Since our previous work[32] has reported that the interactions between *N*-PCCs and protein can be suppressed to avoid the undesired biological response as compared with chitosan, *N*-PCCs nanoparticles could be used as promising nano-vehicles for effectively delivering drug.

Table II. Mean Particle Size and Zeta Potential of Chitosan Nanoparticles and the N-PCCs Nanoparticles

Nanoparticles	Particle size (nm)	Polydispersity index	Zeta potential (mV)
Chitosan	165.2 ± 1.9	0.319 ± 0.016	41.9 ± 0.9
N-PCCs16	64.9 ± 2.2	0.316 ± 0.026	27.0 ± 2.1
N-PCCs27	86.7 ± 2.8	0.361 ± 0.013	22.9 ± 2.1
N-PCCs42	119.3 ± 2.4	0.268 ± 0.004	18.4 ± 1.3

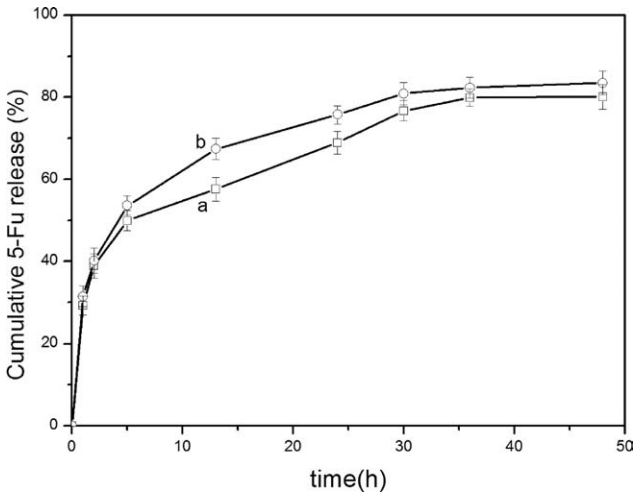

Figure 8. Release of 5-Fu from (a) chitosan nanoparticles and (b) *N*-PCCs27 nanoparticles in PBS at 37.0°C.

CONCLUSIONS

Novel water-soluble biomimetic chitosan derivatives conjugating with zwitterionic PC in different degree of substitution were successfully synthesized through Atherton-Todd reaction under mild conditions. All these *N*-PCCs with decreased crystallization showed excellent solubility in the aqueous solutions within a wide pH range (1–12), but their thermal stability decreased. *N*-PCCs nanoparticles with the decreased particle size and zeta potential value could be still formed in a spherical shape by ionically crosslinking. And *N*-PCCs nanoparticles exhibited similar drug loading and *in vitro* release behaviors as chitosan nanoparticles. The results revealed that *N*-PCCs nanoparticles could be used as promising nanocarriers for drug delivery.

ACKNOWLEDGMENTS

Financial support provided by: National Natural Science Foundation of China (grant numbers: 20504018 and 31040027); Research Development and Innovation Fund of Jinan University (grant number: 21611410).

REFERENCES

1. RaviKumar, M. N. V.; Muzzarelli, R. A. A.; Muzzarelli, C.; Sashiwa, H.; Domb, A. *J. Chem. Rev.* **2004,** *104*, 6017.
2. Janes, K. A.; Calvo, P.; Alonso, M. *J. Adv. Drug Delivery Rev.* **2001,** *47*, 83.
3. Kim, T. H.; Park, I. K.; Nah, J. W.; Choi, Y. J.; Cho, C. S. *Biomaterials* **2004,** *25*, 3783.
4. Xu, T.; Xin, M. H.; Li, M. C.; Huang, H. L.; Zhou, S. Q. *Carbohydr. Polym.* **2010,** *81*, 931.
5. Jia, Z. S.; Shen, D. F.; Xu, W. L. *Carbohydr. Res.* **2001,** *333*, 1.
6. Zhu, A. P.; Chen, T.; Yuan, L. H.; Wu, H.; Lu, P. *Carbohydr. Polym.* **2006,** *66*, 274.
7. Bernkop-Schnürch, A.; Hornof, M.; Guggi, D. *Eur. J. Pharm. Biopharm.* **2004,** *57*, 9.
8. Nishimura, S.; Kai, H.; Shinada, K.; Yoshida, T.; Tokura, S.; Kurita, K.; Nakashima, H.; Yamamoto, N.; Uryu, T. *Carbohydr. Res.* **1998,** *306*, 427.
9. Kong, X.; Li, X.; Wang, X.; Liu, T.; Gu, Y.; Guo, G.; Luo, F.; Zhao, X.; Wei, Y.; Qian, Z. *Carbohydr. Polym.* **2010,** *79*, 170.
10. van der Merwe, S. M.; Verhoef, J. C.; Verheijden, J. H. M.; Kotzé, A. F.; Junginger, H. E. *Eur. J. Pharm. Biopharm.* **2004,** *58*, 225.
11. Kato, Y.; Onishi, H.; Machida, Y. *Biomaterials* **2004,** *25*, 907.
12. Hayward, J. A.; Chapman, D. *Biomaterials* **1984,** *5*, 135.
13. Ishihara, K.; Oshida, H.; Endo, Y.; Ueda, T.; Watanabe, A.; Nakabayashi, N. *J. Biomed. Mater. Res.* **1992,** *26*, 1543.
14. Chapman, D. *Langmuir* **1993,** *9*, 39.
15. Iwasaki, Y.; Aiba, Y.; Morimoto, N.; Nakabayashi, N.; Ishihara, K. J. *Biomed. Mater. Res.* **2000,** *52*, 701.
16. Palmer, R. R.; Lewis, A. L.; Kirkwood, L. C.; Rose, S. F.; Lloyd, A. W.; Vick, T. A.; Peter, P. W.; Stratford, W. *Biomaterials* **2004,** *4*, 785.
17. Chim, Y. T. A.; Lam, J. K. W.; Ma, Y.; Armes, S. P.; Lewis, A. L.; Roberts, C. J.; Stolink, S.; Tendler, S. J. B.; Davies, M. C. *Langmuir* **2005,** *21*, 3591.
18. Lam, J. K. W.; Ma, Y.; Armes, S. P.; Lewis, A. L.; Baldwin, T.; Stolink, S. *J. Controlled Release* **2004,** *100*, 293.
19. Tiera, M. J.; Qiu, X. P.; Bechaouch, S.; Shi, Q.; Fernandes, J. C.; Winnik, F. M. *Bimacromolecules* **2006,** *7*, 3151.
20. Meng, S.; Liu, Z.; Zhong, W.; Wang, Q.; Du, Q. *Carbohydr. Polym.* **2007,** *70*, 82.
21. Zeng, R.; Fu, H.; Zhao, Y. F. *Macromol. Rapid Commun.* **2006,** *27*, 548.
22. Huang, L.; Sui, W.; Wang, Y.; Jiao, Q. *Carbohydr. Polym.* **2010,** *80*, 168.
23. Nishmura, S. J.; Kohgo, O.; Kurita, K. *Macromolecules* **1991,** *24*, 4745.
24. Calvo, P.; Remunan-Lopez, C.; Vila-Jato, J. L.; Alonso, M. J. *J. Appl. Polym. Sci.* **1997,** *63*, 125.
25. Prabaharan, M.; Reis, R. L.; Mano, J. F. *React. Funct. Polym.* **2007,** *67*, 43.
26. Binder, H.; Anikin, A.; Kohlstrunk, B.; Klose, G. J. *Phys. Chem. B* **1997,** *101*, 6618.
27. Satio, H.; Tabeta, R.; Ogawa, K. *Macromolecules* **1987,** *20*, 2424.
28. Tien, C. L.; Lacroix, M.; Ispas-Szabo, P.; Mateescu, M. J. *Controlled Release* **2003,** *93*, 1.
29. Zhang, C.; Ping, Q.; Zhang, H.; Shen, J. *Eur. Polym. J.* **2003,** *39*, 1629.
30. Ma, G. P.; Yang, D. Z.; Zhou, Y. S.; Xiao, M.; Kennedy, J. F.; Nie, J. *Carbohydr. Polym.* **2008,** *74*, 121.
31. Silva, G. A.; Ducheyne, P.; Reis, R. L. *J. Tissue Eng. Regen. M* **2007,** *1*, 4.
32. Wang, Z. H.; Zeng, R.; Tu, M.; Zhao, J. H. *Mater. Lett.* **2012,** *77*, 38.